

Coordinates with Non-Singular Curvature for a Time Dependent Black Hole Horizon

James Lindesay*

Computational Physics Laboratory
Howard University, Washington, D.C. 20059

Abstract

A naive introduction of a dependency of the mass of a black hole on the Schwarzschild time coordinate results in singular behavior of curvature invariants at the horizon, violating expectations from complementarity. If instead a temporal dependence is introduced in terms of a coordinate akin to the river time representation, the Ricci scalar is nowhere singular away from the origin. It is found that for a shrinking mass scale due to evaporation, the null radial geodesics that generate the horizon are slightly displaced from the coordinate singularity. In addition, a changing horizon scale significantly alters the form of the coordinate singularity in diagonal (orthogonal) metric coordinates representing the space-time. A Penrose diagram describing the growth and evaporation of an example black hole is constructed to examine the evolution of the coordinate singularity.

1 Introduction

There is a considerable interest[1, 2] in understanding details of the evaporation of black holes. The singular behavior of Schwarzschild coordinates near the horizon makes those coordinates inconvenient for describing the functional dependencies of relevant physical parameters. One expects that a freely falling observer should not encounter any particularly singular behavior as the horizon is traversed, since that observer's coordinates manifest no singular behavior at the Schwarzschild horizon. Therefore, it

*e-mail address, jlslac@slac.stanford.edu

is useful to develop coordinates that describe an evolution without introducing invariant singular behavior at the horizon.

Braunstein[3] has examined the constraints placed on the form of a conserved energy-momentum tensor in a spherically symmetric geometry, and shown that it must be singular at the coordinate singularity associated with the event horizon using his coordinates. The author agrees that there can be component singularities associated with this tensor due to a particular coordinate representation, but believes that any true singularity associated with physical scalars violates the principles of complementarity and equivalence when one compares the perspectives of fiducial (fixed r, θ, ϕ) vs. freely falling observers. Generally, coordinates are constructed to conveniently represent relationships between events in particular frames of reference, so that any singularities in scalar physical parameters should be associated with local physical content. If there were curvature singularities associated with a slowly evaporating event horizon, one would expect tidal effects producing a type of “brick wall”, which is physically unappealing.

Since the spatio-temporal behavior of Schwarzschild coordinates near the Schwarzschild radius are particularly singular, the anomalous singular behavior due to those coordinates could be eliminated by using a different time coordinate to describe the shrinking mass scale. Such a time coordinate is introduced in section 3 based on the non-orthogonal coordinates of the river model for black holes[4]. This time, which in a manner similar to that of Schwarzschild corresponds to the time of an asymptotic observer, has a behavior near the horizon that does not introduce new singular behavior in relevant scalar functional forms. Orthogonal coordinates will be developed so that intuitive spatio-temporal relationships can be associated with the evolution of a black hole. The behavior of coordinate measures near the coordinate singularity is found to be significantly altered by any non-vanishing temporal dependency $\dot{M} \neq 0$ in section 3.2. A significant consequence of temporal dependency is that the horizon is slightly displaced from the coordinate singularity, as will be explored in section 3.4. To illustrate this displacement, a Penrose diagram for an example black hole is constructed. In addition, holographic arguments are explored to estimate the temperature associated with the evaporation process. Finally, the dynamics of a scalar field is examined, and a temporally slowly varying solution is briefly explored.

2 Temporal Dependence of Schwarzschild Mass Scale

The Schwarzschild geometry is known to describe a spherically symmetric static space-time. It is of interest to examine the geometry generated by naively giving a dependency of the Schwarzschild mass scale on the Schwarzschild time parameter t_S

$$R_M \equiv \frac{2G_N M(ct_S)}{c^2} = R_S. \quad (2.1)$$

The Schwarzschild radius is directly determined by the mass scale, and for clarity will be labeled by R_M . For a metric form given by

$$ds^2 = -\left(1 - \frac{R_M(ct_S)}{r}\right)(dct_S)^2 + \frac{dr^2}{1 - \frac{R_M(ct_S)}{r}} + r^2(d\theta^2 + \sin^2\theta d\phi^2) \quad (2.2)$$

the non-vanishing affine connections (with $x_S^0 \equiv ct_S$) are

$$\begin{aligned} \Gamma_{00}^0 &= -\frac{\dot{R}_M}{2(r-R_M)}, & \Gamma_{0r}^0 &= \frac{1}{2r} \left(\frac{R_M}{r-R_M} \right), & \Gamma_{rr}^0 &= \frac{r^2 \dot{R}_M}{2(r-R_M)^3}, \\ \Gamma_{00}^r &= \frac{R_M(r-R_M)}{2r^3}, & \Gamma_{0r}^r &= \frac{\dot{R}_M}{2(r-R_M)}, & \Gamma_{rr}^r &= -\frac{1}{2r} \left(\frac{R_M}{r-R_M} \right), \\ \Gamma_{\theta\theta}^r &= -(r-R_M), & \Gamma_{\phi\phi}^r &= -(r-R_M) \sin^2\theta, & \Gamma_{r\theta}^\theta &= \frac{1}{r}, \\ \Gamma_{\phi\phi}^\theta &= -\cos\theta \sin\theta, & \Gamma_{r\phi}^\phi &= \frac{1}{r}, & \Gamma_{\theta\phi}^\phi &= \cot\theta. \end{aligned} \quad (2.3)$$

A comparison of geodesic motion from rest allows a determination of the proper acceleration associated with a fixed (fiducial) observer

$$a_{proper} = \frac{R_M c^2}{2r^2} \sqrt{\frac{r}{r-R_M}}, \quad (2.4)$$

which is seen to be singular at $r = R_M$.

The Ricci tensor takes the form

$$((\mathcal{R}_{\mu\nu})) = \begin{pmatrix} \frac{2\dot{R}_M^2 + (r-R_M)\ddot{R}_M}{2(r-R_M)^2} & -\frac{\dot{R}_M}{r(r-R_M)} & 0 & 0 \\ -\frac{\dot{R}_M}{r(r-R_M)} & -\frac{r^2(2\dot{R}_M^2 + (r-R_M)\ddot{R}_M)}{2(r-R_M)^4} & 0 & 0 \\ 0 & 0 & 0 & 0 \\ 0 & 0 & 0 & 0 \end{pmatrix}. \quad (2.5)$$

In these expressions, the dots represent derivatives with respect to ct_S . Several components of the Ricci tensor are seen to be singular at the coordinate singularity $r = R_M$. Of more significance, the Ricci scalar

$$\mathcal{R} = -\frac{r(2\dot{R}_M^2 + (r - R_M)\ddot{R}_M)}{2(r - R_M)^3} \quad (2.6)$$

is seen to be singular at the coordinate singularity for non-vanishing \dot{R}_M . The (mixed) Einstein tensor given by

$$((\mathcal{G}^\nu_\mu)) = \begin{pmatrix} 0 & \frac{\dot{R}_M}{(r - R_M)^2} & 0 & 0 \\ -\frac{\dot{R}_M}{r^2} & 0 & 0 & 0 \\ 0 & 0 & \frac{r(2\dot{R}_M^2 + (r - R_M)\ddot{R}_M)}{2(r - R_M)^3} & 0 \\ 0 & 0 & 0 & \frac{r(2\dot{R}_M^2 + (r - R_M)\ddot{R}_M)}{2(r - R_M)^3} \end{pmatrix} \quad (2.7)$$

is likewise seen to manifest this singular behavior at $r = R_M$.

Einstein equations can be used to examine the behavior of any energy-momentum densities:

$$\mathcal{G}_{\mu\nu} = \mathcal{R}_{\mu\nu} - \frac{1}{2}g_{\mu\nu}\mathcal{R} = -\frac{8\pi G_N}{c^4}\mathcal{T}_{\mu\nu}. \quad (2.8)$$

The curvature scalar is associated with the trace of the energy-momentum tensor

$$\mathcal{R} = \frac{8\pi G_N}{c^4}g^{\mu\nu}\mathcal{T}_{\mu\nu}. \quad (2.9)$$

The Ricci scalar \mathcal{R} should be non-singular at $r = R_M$ if the coordinate R_M is only a coordinate anomaly. Singularities introduced into components of physical parameters due to coordinate transformations $\mathcal{T}_{\hat{\mu}\hat{\nu}} = \frac{\partial x^\alpha}{\partial \hat{x}^{\hat{\mu}}}\mathcal{T}_{\alpha\beta}\frac{\partial x^\beta}{\partial \hat{x}^{\hat{\nu}}}$ have a different significance from those associated with invariant physical content. The singular behavior of the scalar \mathcal{R} at $r = R_M$ for non-vanishing \dot{R}_M represents a singular structure associated with the local space-time that must be reflected in the physical content as shown in Eq. 2.9, and for this scalar function is independent of the particular coordinate description.

3 A Singularity-free Horizon

3.1 The river model

The so called ‘‘river model’’ has been explored by several authors[4, 5]

to gain insight into the dynamics of horizons. The metric takes an off-diagonal form generically given by

$$ds^2 = -(dct_R)^2 + [dr - \beta(r)dct_R]^2 + r^2(d\theta^2 + \sin^2\theta d\phi^2). \quad (3.1)$$

The “speed” β has been interpreted by some to be the speed of radial outflow of the space-time “river” through which objects move using the rules of special relativity[4]. The transformation

$$ct_R = ct_* - \int^r \frac{\beta(r')}{1 - \beta^2(r')} dr' \quad (3.2)$$

diagonalizes the metric, giving the form

$$ds^2 = -(1 - \beta^2(r))(dct_*)^2 + \frac{dr^2}{1 - \beta^2(r)} + r^2(d\theta^2 + \sin^2\theta d\phi^2). \quad (3.3)$$

The river speed becomes luminal at the horizon associated with the (ct_*, r) coordinates.

For the present examination, the metric will take the form

$$ds^2 = -\left(1 - \frac{R_M(ct_R)}{r}\right) (dct_R)^2 + 2\sqrt{\frac{R_M(ct_R)}{r}} dct_R dr + dr^2 + r^2 d\omega^2 \quad (3.4)$$

where $d\omega^2 \equiv d\theta^2 + \sin^2\theta d\phi^2$. This space-time asymptotically corresponds with Minkowski space similar to (but not necessarily identical to) the behavior of a Schwarzschild geometry. The non-vanishing affine connections ($x^0 \equiv ct_R$) are given by

$$\Gamma_{00}^r = \frac{1}{2r} \left[\left(\frac{R_M}{r}\right) - \left(\frac{R_M}{r}\right)^2 + \dot{R}_M \left(\frac{r}{R_M}\right)^{1/2} \right],$$

$$\begin{aligned}
\Gamma_{00}^0 &= \frac{1}{2r} \left(\frac{R_M}{r} \right)^{3/2}, & \Gamma_{0r}^0 &= \frac{1}{2r} \left(\frac{R_M}{r} \right), & \Gamma_{rr}^0 &= \frac{1}{2r} \left(\frac{R_M}{r} \right)^{1/2}, \\
\Gamma_{\theta\theta}^0 &= -r \left(\frac{R_M}{r} \right)^{1/2}, & \Gamma_{\phi\phi}^0 &= -r \left(\frac{R_M}{r} \right)^{1/2} \sin^2\theta, \\
\Gamma_{0r}^r &= -\frac{1}{2r} \left(\frac{R_M}{r} \right)^{3/2}, & \Gamma_{rr}^r &= -\frac{1}{2r} \left(\frac{R_M}{r} \right), \\
\Gamma_{\theta\theta}^r &= -(r - R_M), & \Gamma_{\phi\phi}^r &= -(r - R_M) \sin^2\theta, \\
\Gamma_{r\theta}^\theta &= \frac{1}{r}, & \Gamma_{\phi\phi}^\theta &= -\cos\theta \sin\theta, \\
\Gamma_{r\phi}^\phi &= \frac{1}{r}, & \Gamma_{\theta\phi}^\phi &= \cot\theta.
\end{aligned} \tag{3.5}$$

The mixed Einstein tensor

$$((\mathcal{G}_\mu^\nu)) = \begin{pmatrix} 0 & 0 & 0 & 0 \\ -\frac{\dot{R}_M}{r^2} & -\frac{\dot{R}_M}{R_M r} \sqrt{\frac{R_M}{r}} & 0 & 0 \\ 0 & 0 & -\frac{\dot{R}_M}{4R_M r} \sqrt{\frac{R_M}{r}} & 0 \\ 0 & 0 & 0 & -\frac{\dot{R}_M}{4R_M r} \sqrt{\frac{R_M}{r}} \end{pmatrix} \tag{3.6}$$

is seen to be non-singular away from $r = 0$. Likewise, the Ricci scalar

$$\mathcal{R} = \frac{3\dot{R}_M}{2r^2} \sqrt{\frac{r}{R_M}} \tag{3.7}$$

is non-singular away from a physical singularity at the origin. This represents the key point of appeal of this approach. The invariant curvature (and any related invariant physical parameter) is nowhere singular away from the origin. Any coordinate singularities manifest only in components unique to that particular coordinate representation.

3.2 Diagonalization of metric form for a dynamic mass scale

The construction of orthogonal temporal-radial coordinates is appealing, especially with regards to one's intuitive use of the coordinates. If one attempts a coordinate transformation of the form

$$dct_R = A(ct_R, r) dct_D + \Delta(ct_R, r) dr \quad , \quad dr_R = dr, \tag{3.8}$$

the function Δ can be chosen to immediately diagonalize the metric in Eq. 3.4 if it is of the form

$$\Delta(ct_R, r) = \frac{\sqrt{\frac{R_M(ct_R)}{r}}}{1 - \frac{R_M(ct_R)}{r}}. \quad (3.9)$$

The diagonalized metric then takes the form

$$ds^2 = -\left(1 - \frac{R_M(ct_R)}{r}\right) A^2(ct_R, r) dct_D^2 + \frac{dr^2}{1 - \frac{R_M(ct_R)}{r}} + r^2(d\theta^2 + \sin^2\theta d\phi^2). \quad (3.10)$$

The transformed temporal coordinate t_D must satisfy

$$\frac{\partial ct_D}{\partial ct_R} = \frac{1}{A(ct_R, r)} \quad , \quad \frac{\partial ct_D}{\partial r} = -\frac{1}{A(ct_R, r)} \left(\frac{\sqrt{\frac{R_M(ct_R)}{r}}}{1 - \frac{R_M(ct_R)}{r}} \right), \quad (3.11)$$

along with the integrability condition

$$\frac{\partial}{\partial r} \log A + \Delta \frac{\partial}{\partial ct_R} \log A = \frac{\partial}{\partial ct_R} \Delta. \quad (3.12)$$

If $\ddot{R}_M = 0$, a solution can be demonstrated for the coordinate transformation. The reduced coordinate ζ will be defined by $\zeta \equiv \frac{R_M}{r}$. The coefficient A is assumed to approach unity for vanishing \dot{R}_M , giving the usual static Schwarzschild coordinates. It is convenient to assume a form for this coefficient

$$\log A(ct_R, r) = F(\zeta) \dot{R}_M. \quad (3.13)$$

The integrability condition Eq. 3.12 gives the equation

$$\frac{\partial}{\partial \zeta} F(\zeta) = \frac{\frac{\partial \Delta}{\partial \zeta}}{\dot{R}_M \Delta - \zeta} \quad \text{for} \quad \ddot{R}_M = 0. \quad (3.14)$$

Defining a finite coordinate (ct_{R_o}, r_o) , the coefficient A then satisfies

$$A(ct_R, r) = A(ct_R, r_o) \exp \int_{\zeta(ct_R, r_o)}^{\zeta(ct_R, r)} \left[\frac{\frac{\partial \Delta(\tilde{\zeta})}{\partial \tilde{\zeta}} \dot{R}_M d\tilde{\zeta}}{\Delta(\tilde{\zeta}) \dot{R}_M - \tilde{\zeta}} \right],$$

$$A(ct_R, r_o) = \exp \int_{\zeta(ct_{R_o}, r_o)}^{\zeta(ct_R, r_o)} \left[\frac{\frac{\partial \Delta(\tilde{\zeta})}{\partial \tilde{\zeta}} \dot{R}_M d\tilde{\zeta}}{\Delta(\tilde{\zeta}) \dot{R}_M - \tilde{\zeta}} \right], \quad (3.15)$$

where the constant $A(ct_{R_o}, r_o)$ is chosen to satisfy correspondence between river and orthogonal coordinates independent of the value of \dot{R}_M . Near the coordinate singularity $\zeta \rightarrow 1$, the function $\Delta(\zeta)$ from Eq. 3.9 becomes singular and the temporal coefficient A is seen to be likewise singular $A \rightarrow \frac{1}{1-\zeta}$. Examining the metric form in Eq. 3.10, this suggests that a changing radial mass scale $\dot{R}_M \neq 0$ significantly alters the form of the coordinate singularity in the diagonal coordinates. For instance, the transformation to a radial conformal coordinate $d\Pi = \frac{dr}{\left(1 - \frac{R_M}{r}\right)A(ct_R, r)}$ is seen to be non-singular at the coordinate singularity in these coordinates unless $\dot{R}_M = 0$ (in which case it becomes the radial tortoise coordinate).

3.3 Radial proper distance and acceleration

A measurement of radial proper distance involves the determination of the distance between radially separated regions at simultaneous times in orthogonal temporal-radial coordinates. In such coordinates a direct interpretation can be given for distant simultaneous measurements as well as temporal measurements at a fixed spatial position. From calculations in Eq. 3.10, this is seen to be given by

$$d\rho = \frac{dr}{\sqrt{1 - \frac{R_M}{r}}}. \quad (3.16)$$

This formula applies external to the coordinate singularity $r = R_M$. Geodesic radial motion from rest can be determined using the connections previously calculated;

$$\frac{d^2r}{dc\tau^2} + \frac{1}{2r} \left[\frac{R_M}{r} + \left(\frac{\dot{R}_M}{1 - \frac{R_M}{r}} \right) \left(\frac{r}{R_M} \right)^{1/2} \right] = 0, \quad (3.17)$$

$$\frac{d^2ct_R}{dc\tau^2} + \frac{1}{2r} \left(\frac{R_M}{r} \right)^{3/2} \left(\frac{1}{1 - \frac{R_M}{r}} \right) = 0, \quad (3.18)$$

which is useful for determination of the proper acceleration near the coordinate singularity. The proper acceleration of a static fiducial observer located at (r, θ, ϕ) can be calculated using Eqns. 3.16 and 3.17, giving

$$a_{proper} = \frac{R_M c^2}{2r^2} \sqrt{\frac{r}{r - R_M}} \left(1 + \frac{r^2 \dot{R}_M}{(r - R_M) R_M} \left(\frac{r}{R_M} \right)^{1/2} \right). \quad (3.19)$$

For a slowly evaporating black hole, this form is seen to imply a vanishing proper acceleration at a value approximately given by $R_M/(1 + \dot{R}_M)$.

3.4 Evolution of the horizon and mass scale

A black hole horizon is a light-like surface corresponding to a finite area of radially “outgoing” null geodesics. In a static Schwarzschild geometry, these null geodesics maintain a fixed finite radial coordinate away from the physical singularity at $r = 0$. The general form for null radial geodesics in the dynamic geometry specified in Eq. 3.4 is given by

$$\frac{dr_\gamma}{dct_R} = -\sqrt{\frac{R_M}{r_\gamma}} \pm 1. \quad (3.20)$$

Outgoing photons (r_γ increases with ct_R) traverse trajectories that correspond to the upper sign. The radial coordinate of a *dynamic* horizon must satisfy

$$\frac{dR_H}{dct_R} = -\sqrt{\frac{R_M}{R_H}} + 1 \quad , \quad R_H = \frac{R_M}{(1 - \dot{R}_H)^2} \quad . \quad (3.21)$$

This equation defines the temporal behavior of the horizon as the radial mass scale R_M varies. Unlike the case for the static geometry, the horizon here is not given by the radial mass scale $R_H \neq R_M$, since photons instantaneously located at the radial mass scale R_M are momentarily stationary in r , while the horizon is not. The horizon is the outermost set of null geodesics that satisfy Eq. 3.21 without reaching outgoing null infinity \mathcal{I}^+ . Photons with $r_\gamma > R_H$, $\dot{r}_\gamma > \dot{R}_H$ will escape the singularity at $r = 0$ (even if $r_\gamma < R_M$). This is the reason that care has been taken to differentiate between the terms Schwarzschild radius, radial mass scale, horizon, and coordinate singularity.

For completeness, the behavior of a radially infalling spherical light-like shell is given by

$$\frac{dR_{sh}}{dct_R} = -\sqrt{\frac{R_M}{R_{sh}}} - 1 \quad , \quad R_{sh} = \frac{R_M}{(1 + \dot{R}_{sh})^2} \quad . \quad (3.22)$$

These relations will be helpful in the construction of a model black hole that forms at a finite time from energy collapse, then evaporates away, as developed in section 3.6.

3.5 Holographic considerations

Thermodynamic estimates can be made using holographic arguments relating the horizon to entropy. The entropy associated with a horizon of area A will be assumed to satisfy

$$S = k_B \frac{A}{4G_N} \frac{c^3}{\hbar} = k_B \frac{\pi R_H^2}{G_N} \frac{c^3}{\hbar}. \quad (3.23)$$

Since the dominant form of the energy is assumed to be due to the mass of the black hole, the energy U will be taken to be

$$U = Mc^2 = \frac{c^4}{2G_N} R_M = \frac{c^4}{2G_N} R_H (1 - \dot{R}_H)^2. \quad (3.24)$$

For the present, it will be assumed that any “pressure” contribution to the thermodynamics of the geometry is negligible compared to the entropic contribution. In this case, the temperature of the black hole is given by

$$T = \frac{dU}{dS} = \frac{\hbar c}{4\pi k_B} \left[\frac{(1 - \dot{R}_H)^2}{R_H} + 2(1 - \dot{R}_H) \frac{d\dot{R}_H}{dR_H} \right]. \quad (3.25)$$

External to the region for which $\dot{R}_M \sim 1 - \frac{R_M}{r}$, the geometry behaves very similarly to a Schwarzschild space-time. Therefore, an estimation of the evaporation rate will be made using the (not too) near R_M behavior of fields in Schwarzschild geometry. Massless particles near the coordinate singularity encounter an effective potential barrier[6], with the s-wave barrier height of the order $U_{barrier} \sim \frac{\hbar c}{R_M}$ and range $\sim \frac{3}{2} R_M$. The average energy of the thermal quanta is of order $\sim k_B T$, with an expected average rate of quanta over the energy barrier of order $\sim U_{barrier}/\hbar$. Therefore the rate of evaporation can be estimated by $\dot{M}c^2 = \frac{c^4}{2G_N} \dot{R}_M \sim -\frac{k_B T}{\hbar c} \frac{U_{barrier}}{\hbar} \sim -\frac{\hbar c}{R_M^2}$, which means that $\dot{R}_M \sim -\left(\frac{L_P}{R_M}\right)^2$, $|\dot{R}_M| \ll 1$ (where L_P is the Planck length $L_P^2 \equiv \hbar G_N/c^3 = (\hbar/M_{PC})^2$). This implies that $\frac{d\dot{R}_H}{dR_H} \sim \frac{1}{R_M} \left(\frac{L_P}{R_M}\right)^2 \ll \frac{1}{R_M}$, which means that the temperature given in Eq. 3.25 is dominated by the first term in the bracket.

To check the consistency of the assumption of the entropic domination of thermodynamic energy, in the first law of thermodynamics $dU = T dS - P dV$ the “pressure” term can be estimated to be of order $\sim \mathcal{T}_r^r 4\pi r^2 dr \sim \dot{M}c^2 dr \sim \frac{\hbar c}{R_M} \frac{dr}{R_M}$, while the entropy term is estimated using Eq. 3.25 to be $T dS \sim \frac{\hbar c}{L_P} \frac{dr}{L_P}$, which clearly dominates the pressure term for horizons beyond the Planck scale.

3.6 Evolution of a spherically symmetric neutral black hole

It is of interest to examine the global structure of a growing and evaporating black hole. In a Penrose diagram, the space-time structure is represented using conformal coordinates (with light-like curves represented by lines with slope ± 1) and the entire space-time mapped onto a finite diagram. It is not useful to construct a relevant separate finite Penrose diagram for a system with constant \dot{R}_M , since all points are contained within the coordinate singularity for either very late or very early times. However one should be able to patch together diagrams for a mass scale that initially grows, then later evaporates away. Consider an infalling spherically symmetric photon shell that contains an energy $M_o c^2$. The region interior to this shell is essentially flat by Birkoff's theorem for spherically symmetric geometries, while the exterior region satisfies the geometry associated with a spherically symmetric mass distribution until that mass evaporates away. All elements of the infalling shell will eventually cross the surface bounding the region for which any outgoing light would eventually hit a singularity at $r = 0$.

The Penrose diagram in Figure 1 demonstrates the expected global structure of such a space-time corresponding to an initially flat (Minkowski) geometry with a radially infalling photon shell of total energy $M_o c^2$. The thick band originating at \mathcal{I}^- represents that photon shell, and the region beneath that band (interior to the shell) has negligible curvatures due to Birkoff's theorem. This lower triangular region is bounded on the left by the time-like curve representing $r = 0$. Since the photon shell will eventually reach $r = 0$ forming a physical singularity, there will be a light-like surface representing the innermost set of out-going photons that can escape eventually hitting the singularity which forms (indicated by the jagged horizontal line on the diagram). This light-like surface is the horizon associated with the black hole, and it is seen to be globally defined, having a non-vanishing radial coordinate $R_H > 0$ even prior to the space-time point(s) when the infalling photon shell crosses this horizon. However, the radial mass scale R_M associated with the coordinate singularity in the highly curved metric of the black hole geometry is seen to increase from a vanishing value to that appropriate to a Schwarzschild-like space-time as the photons in the shell cross this growing coordinate. As elements of the

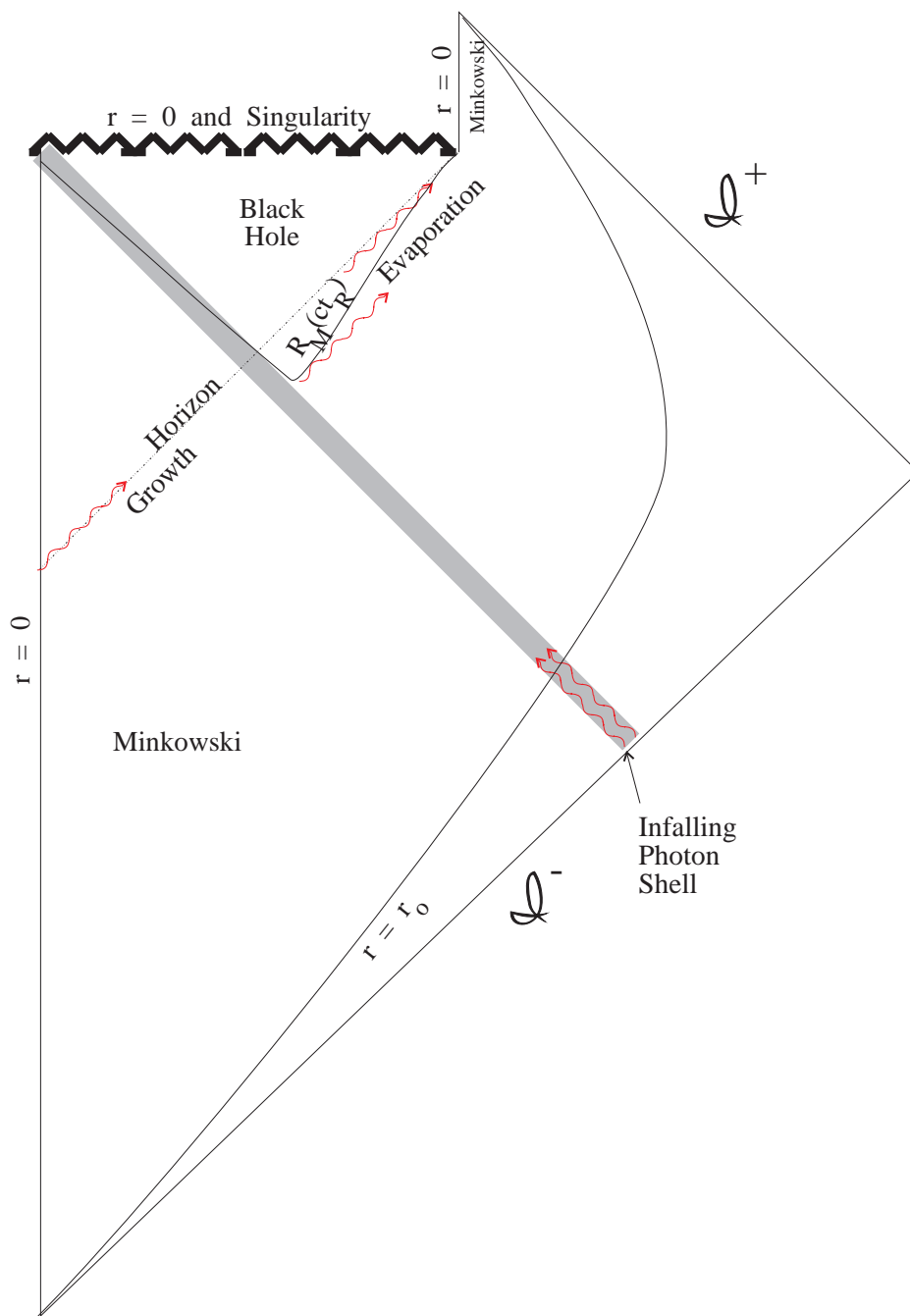


Figure 1: Penrose diagram for formation and evaporation of a spherically symmetric neutral black hole

photon shell reach $r = 0$, the curve $r = 0 (< R_M)$ interior to the coordinate singularity becomes the space-like singularity of increasing strength represented by the initiation of the jagged curve. The width of this shell represents the duration of the period of growth in the radial mass scale R_M . Increases in R_M are associated with local infalling shell photons as they cross growing “horizon” scales (any of which would represent the global horizon were the growth to stop at that stage), and the curve $R_M(ct_R)$ grows away from the physical singularity at $r = 0$ after the initial edge of the infalling photon shell initiates this singularity. In the space-time region for which the curved coordinates are of relevance, the curve $r = 0$ therefore tracks a physical singularity with an associated mass scale $R_M \neq 0$. The expected difference between the curve $R_M(ct_R)$ and the horizon R_H has been exaggerated for emphasis. This difference is determined by the relation for the light-like curve given in Eq. 3.21. The curve $R_M(ct_R)$ crosses the global horizon R_H when $\dot{R}_H = 0$, during which the rate of mass growth is comparable to that of mass loss due to radiation. If the energy influx rate were to exactly match the evaporation rate for an extended period, the geometry would be expected to represent an essentially static Schwarzschild space. For the case being examined, as demonstrated in section 3.4 a photon emitted from R_M is able to escape hitting the singularity because of the shrinking of the mass scale due to evaporation. Since R_M is associated with the curved metric, radial coordinates relative to R_M are determined relative to the jagged singularity $r = 0$. During growth, the coordinate singularity R_M has a value less than the radial coordinate of the horizon, whereas during evaporation the horizon has radial coordinate less than the radial mass scale $R_H < R_M$. The physical singularity $r = 0$ and the coordinate singularity R_M are seen to vanish together, leaving a (shifted) time-like curve $r = 0$ associated with the final low curvature Minkowski-like space-time, represented as the upper triangular region in the diagram subsequent to complete evaporation of the singularity.

From thermodynamic (first law) arguments, one expects substantial modification from the entropic dominated evaporation as R_H approaches the Planck scale. During all periods with non-vanishing radial mass scale, the singularity at $r = 0$ is a physical (space-like) singularity hidden by the horizon R_H , which during evaporation likewise lies within the coordinate singularity R_M . The physical singularity vanishes as $R_M \rightarrow 0$, just as the horizon vanishes $R_H \rightarrow 0$.

3.7 Scalar wave equation

For completeness, the behavior of a free massless scalar field in a geometry appropriately parameterized by functional dependencies in (ct_R, r, θ, ϕ) will next be explored. The action will be assumed to take the form

$$\mathcal{W} = \frac{1}{2} \int g^{\mu\nu} \partial_\mu \chi^* \partial_\nu \chi \sqrt{-g} dx^0 dx^1 dx^2 dx^3. \quad (3.26)$$

Substituting the decomposition $\chi = \sum_{\ell m} \frac{\psi_\ell(ct_R, r)}{r} Y_\ell^m(\theta, \phi)$ results in a dynamical equation of the form

$$\begin{aligned} & -\frac{\partial^2 \psi_\ell}{(\partial ct_R)^2} + \frac{\partial}{\partial ct_R} \left[\sqrt{\frac{R_M}{r}} \left(\frac{\partial \psi_\ell}{\partial r} \right) \right] + \frac{\partial}{\partial r} \left[\sqrt{\frac{R_M}{r}} \left(\frac{\partial \psi_\ell}{\partial ct_R} \right) \right] + \\ & \frac{\partial}{\partial r} \left[\left(1 - \frac{R_M}{r} \right) \left(\frac{\partial \psi_\ell}{\partial r} \right) \right] - \left[\frac{\ell(\ell+1) + \frac{R_M}{r}}{r^2} + \frac{1}{r} \frac{\partial}{\partial ct_R} \sqrt{\frac{R_M}{r}} \right] \psi_\ell = 0. \end{aligned} \quad (3.27)$$

In the special case of steady growth or evaporation $\ddot{R}_M = 0$, this equation admits a (temporally) slowly varying solution in terms of the variable $\zeta \equiv \frac{R_M(ct_R)}{r}$ that will be briefly discussed. Substituting this variable dependency, Eq. 3.27 takes the form

$$\begin{aligned} & \left[-\dot{R}_M^2 - 2\dot{R}_M \zeta^{3/2} + (1 - \zeta) \zeta^2 \right] \frac{\partial^2 \psi_\ell}{\partial \zeta^2} + \left[-3\dot{R}_M \zeta^{1/2} + 2\zeta - 3\zeta^2 \right] \frac{\partial \psi_\ell}{\partial \zeta} + \\ & - \left[\ell(\ell + 1) + \zeta + \frac{1}{2} \dot{R}_M \zeta^{-1/2} \right] \psi_\ell = 0. \end{aligned} \quad (3.28)$$

This field has a near-horizon ($r \rightarrow R_M, \zeta \rightarrow 1$) form given by $\psi_\ell^H(\zeta) \approx \psi_\ell^H(1) \exp([\ell(\ell + 1) + 1](1 - \zeta))$, while for an evaporating black hole, the asymptotic (s-wave) behavior $\zeta \rightarrow 0$ with vanishing field density is in the form of a modified Bessel function $\psi_0^\infty(\zeta) \sim \sqrt{\zeta} I_{\frac{2}{3}}\left(\frac{4}{3} \frac{\zeta^{3/4}}{\sqrt{-2\dot{R}_M}}\right)$. If such a field were present in this geometry, its amplitude would have to be of a scale such that its energy density would have a negligible contribution to the space-time geometry in order for this solution to be consistent.

4 Conclusions

A temporal parameter t_R that is not completely orthogonal to the radial parameter has been shown to be adequate for describing the evolution of

the physical parameters associated with a spherically symmetric black hole without introducing invariant singular behavior away from $r = 0$. The coordinate singularity introduced by these asymptotically flat coordinates is slightly displaced from the light-like surface that defines a finite horizon which if crossed insures an eventual meeting with the physical singularity at $r = 0$. During evaporation, this displacement occurs because a radially outgoing photon originating from the coordinate singularity is momentarily at fixed (then increasing) radial coordinate, while the horizon has a slowly decreasing radial scale. This calculated discrepancy between the radial coordinates of the horizon and the coordinate singularity, as well as the modification in the form of the proper acceleration near the horizon, give a natural basis for the scale of a *stretched horizon*, within which there is significant modification of the local physics.

Holographic considerations suggest that the thermodynamics of evaporation is not significantly altered by the temporal dependence. The behavior of a massless scalar field has been examined, and besides the usual quantum modes, a particular solution in terms of the parameter $\zeta = \frac{R_M}{r}$ is admitted in this geometry if $\ddot{R}_M = 0$. The radial coordinate measure of proper scale in these coordinates behaves essentially the same as does that in Schwarzschild coordinates. However, there is a considerable difference in the behavior of the orthogonal temporal coordinate measure t_D to that of Schwarzschild coordinates near the coordinate singularity. This qualitative discrepancy occurs for any non-vanishing value of \dot{R}_M . The transformation relationship between the temporal parameters t_R and t_D demonstrate the introduction of additional singular behavior into the orthogonal coordinate, justifying the preferred use of t_R to describe the physical dynamics.

Acknowledgment

The author gratefully acknowledges Lenny Susskind for teaching him about the subtleties of horizons and black holes. In addition, the author thanks J.D. Bjorken for introducing him to the river model for black holes, and for discussions involving the structure of horizons during black hole formation.

References

- [1] “Production and decay of evolving horizons”, A.B. Nielsen and M. Visser, gr-qc/0510083 (2006) 25 pages, *Classical and Quantum Gravity* 23 (2006) 4637-4658.
- [2] “What, no black hole evaporation?”, P. Hajicek and W. Israel, *Physics Letters* 80A (1980) 9-10.
- [3] Informal discussions with Samuel L. Braunstein, concerning unpublished manuscript “Energy-momentum tensor near the Schwarzschild event horizon”, March-April 2006.
- [4] “The river model of black holes”, A.J.S. Hamilton and J.P. Lisle, gr-qc/0411060 (2004) 14 pages.
- [5] “An Introduction of Multiple Scales in a Dynamical Cosmology”, J.Lindesay, gr-qc/0605007 (2006) 8 pages.
- [6] **An Introduction to Black Holes, Information, and the String Theory Revolution: The Holographic Universe**, L. Susskind and J. Lindesay, Chapters 2 and 5, World Scientific, Singapore (2005)